

$Q' = x_2^2 - x_1^2 = -Q$. So N is a negautomorph of Q . In general, the product of two negautomorphs is an automorph.

Minkowski plane

Consider the two-dimensional space-time spanned by \mathbf{a}_1 and \mathbf{a}_2 . Its points $\mathbf{x} = x_1\mathbf{a}_1 + x_2\mathbf{a}_2$ are called 'events' and have a space and a time coordinate (r, t) . Multiplying the time coordinate by the speed of light c (normalized to 1), it also becomes a space coordinate. So we can put $x_1 = r$, $x_2 = ct = t$. Lorentz transformations L are linear transformations in the space-time leaving the light velocity invariant and thus also the value $x_1^2 - x_2^2$. A light wave propagates along events for which one has $x_1 = \pm x_2$. Accordingly, $\mathbf{a}_1 \pm \mathbf{a}_2$ are called light directions, where \mathbf{a}_1 is along the space axis and \mathbf{a}_2 along the time axis. Note that the metric tensor $g_{11} = \mathbf{a}_1 \circ \mathbf{a}_1 = 1$, $g_{22} = \mathbf{a}_2 \circ \mathbf{a}_2 = -1$, $g_{12} = \mathbf{a}_1 \circ \mathbf{a}_2 = 0$ is left invariant by the Lorentz transformation L which is therefore a hyperbolic rotation of the Minkowski plane. The scaling transformation induced by L along the light cone corresponds to the red shift (dilatation) or to the blue shift (contraction) of a light wave emitted from a moving source.

References

GRÜNBAUM, B. & SHEPARD, G. C. (1987). *Tiling and Pattern*. New York: Freeman.

- HIRSHFELD, F. L. (1968). *Acta Cryst.* **A24**, 301-311.
 JANNER, A. (1986). *J. Phys. (Paris) Colloq.* **47**, C3, 95-102.
 JANNER, A. (1988). In *Fractals, Quasicrystals, Chaos, Knots and Algebraic Quantum Mechanics*, edited by A. AMANN, L. CEDERBAUM, & W. GANS, pp. 93-109. Dordrecht: Kluwer.
 JANNER, A. (1989). *Phase Transitions*, **16/17**, 87-101.
 JANNER, A. (1990a). In *Geometry and Thermodynamics*, edited by J.-C. TOLÉDANO, pp. 49-65. New York: Plenum.
 JANNER, A. (1990b). *Acta Cryst.* **A46**, C448.
 JANNER, A. (1991). *Phys. Rev. B*, **43**, In the press.
 JANNER, A. & ASCHER, E. (1969a). *Z. Kristallogr.* **130**, 277-303.
 JANNER, A. & ASCHER, E. (1969b). *Physica (Utrecht)*, **45**, 33-66.
 JANNER, A. & ASCHER, E. (1969c). *Physica (Utrecht)*, **45**, 67-85.
 JANNER, A. & JANSSEN, T. (1990). In *Quasicrystals and Incommensurate Structures in Condensed Matter*, edited by J. M. YACAMÁN, D. ROMEU, V. CASTAÑO & A. GÓMEZ, pp. 96-108. Singapore: World Scientific.
 JANSSEN, T. (1990). In *Proceedings of the Anniversary Adriatico Research Conference on Quasicrystals*, edited by M. V. JARIĆ & S. LUNDQVIST, pp. 130-143. Singapore: World Scientific.
 JANSSEN, T. & JANNER, A. (1987). *Adv. Phys.* **36**, 519-624.
 KUO, K. H. (1987). *Acta Cryst.* **A43**, C312.
 KUO, K. H. (1990). In *Proceedings of the Anniversary Adriatico Research Conference on Quasicrystals* edited by M. V. JARIĆ & S. LUNDQVIST, pp. 92-108. Singapore: World Scientific.
 MACGILLAVRY, C. H. (1986). In *M. C. Escher, Art and Science*, edited by H. S. M. COXETER, M. EMMER, R. PENROSE & M. L. TEUBER, pp. 69-80. Amsterdam: North-Holland.
 WONDRAUSCHEK, H. (1983). In *International Tables for Crystallography*. Vol. A. *Space-Group Symmetry*, edited by T. HAHN, pp. 711-731. Dordrecht: Kluwer.
 YAMAMOTO, A. (1990). Symposium on Symmetry in Physical Space and in Superspaces. Physical Applications: Quasicrystals, Incommensurate Phases, Châtenay-Malabry, France, 29-31 July 1990.

Acta Cryst. (1991). **A47**, 590-597

Computation of Absorptive Form Factors for High-Energy Electron Diffraction

BY A. WEICKENMEIER AND H. KOHL

Institut für Angewandte Physik, Technische Hochschule Darmstadt, Hochschulstrasse 6, D-6100 Darmstadt, Germany

(Received 30 November 1990; accepted 19 April 1991)

Abstract

An efficient procedure for calculating the contribution of the thermal diffuse scattering to the absorptive form factor is outlined. For an isotropic Einstein model all integrations could be performed analytically by using suitable functions to fit the elastic electron scattering amplitudes. The result is cast into a function subroutine which is available upon request. Computed values are compared with previous calculations and with measurements.

1. Introduction

The quantitative interpretation of electron diffraction patterns requires a comparison of the recorded pat-

terns with calculations (Steeds, 1983). To perform a computation the Fourier coefficients of the lattice potential must be known. In a first approximation one considers only elastic scattering. In practice, however, inelastic processes scatter electrons out of the Bragg reflections into the background causing an attenuation of the reflections. The removal of electrons from the Bragg reflections can be described as an absorption. This absorption together with the increased background very severely affects the contrast in diffraction patterns, especially in the case of high- Z materials. The attenuation of the reflections can be incorporated into the dynamical theory by adding an imaginary part to the crystal potential (Yoshioka, 1957).[†] The calculation of the diffuse back-

ground is more difficult (Rossouw & Bursill, 1986) and will not be attempted here. Thus, if absorption is included, each Fourier coefficient $U_{\mathbf{g}}$ consists of two parts

$$U_{\mathbf{g}} = V_{\mathbf{g}} + iV'_{\mathbf{g}}, \quad (1)$$

where $V_{\mathbf{g}}$ denotes the Fourier coefficient of the (real) lattice potential $V(\mathbf{r})$ and $V'_{\mathbf{g}}$ the absorption arising from inelastic scattering. In the actual computations one must use certain estimates for $V'_{\mathbf{g}}$, since these quantities are very difficult to calculate. Up to now only very rough approximations have been used. For example, Hashimoto, Howie & Whelan (1962) assume that the ratio $V'_{\mathbf{g}}/V_{\mathbf{g}}$ has the constant value of 0.1 for all \mathbf{g} . We show that by applying a simple physical model more realistic estimates of $V'_{\mathbf{g}}$ can be obtained and, moreover, $V_{\mathbf{g}}$ and $V'_{\mathbf{g}}$ can be computed using the same small set of atomic parameters.

An excellent approximation of $V_{\mathbf{g}}$ can readily be obtained by neglecting the influence of binding effects onto the outermost atomic electrons. Then $V_{\mathbf{g}}$ is given by

$$V_{\mathbf{g}} = \frac{4\pi\hbar^2}{2mV_{uc}} \sum_k \exp[-i\mathbf{g}\boldsymbol{\tau}_k] \exp[-M_k g^2] f_k(\mathbf{g}). \quad (2)$$

In this equation V_{uc} denotes the volume of the unit cell, m the rest mass of the electron, \mathbf{g} a reciprocal-lattice vector, $\boldsymbol{\tau}_k$ the position of the atom k in the unit cell and f_k the atomic scattering amplitude in the first-order Born approximation, respectively. The exponent in the Debye-Waller factor is abbreviated as $M_k = \frac{1}{2}\langle u_k^2 \rangle$, where $\langle u_k^2 \rangle$ is the mean square of the thermal displacement of atom k .

The main problem in calculating $U_{\mathbf{g}}$ is the absorptive part, because there are several processes causing absorption. The most important processes are thermal diffuse scattering (TDS), plasma losses and core excitations:

$$V'_{\mathbf{g}} = V'_{\mathbf{g}}(\text{TDS}) + V'_{\mathbf{g}}(\text{Plasma}) + V'_{\mathbf{g}}(\text{Core}). \quad (3)$$

A quantitative calculation of these processes would be very complicated because their solid-state nature has to be taken into account. To avoid this difficulty and to obtain an idea of the influence of absorption on the diffraction patterns one is interested in simple models and calculation procedures.

TDS is the major contribution to $V'_{\mathbf{g}}$, except for V'_0 . Therefore the plasma losses and core excitations are usually neglected

$$V'_{\mathbf{g}} \approx V'_{\mathbf{g}}(\text{TDS}) \text{ if } \mathbf{g} \neq 0. \quad (4)$$

The calculation of the influence of TDS can be simplified by applying the Einstein model. In this approximation the thermal vibrations of individual atoms are statistically independent of each other. This procedure allows one to express $V'_{\mathbf{g}}$ as

$$V'_{\mathbf{g}} = \frac{4\pi\hbar^2}{2mV_{uc}} \sum_k \exp[-i\mathbf{g}\boldsymbol{\tau}_k] \exp[-M_k g^2] f'_k(\mathbf{g}). \quad (5)$$

It should be noticed that $V_{\mathbf{g}}$ and $V'_{\mathbf{g}}$ are given by similar formulas. The only difference is that for the calculation of $V_{\mathbf{g}}$ the atomic elastic scattering amplitude $f(\mathbf{g})$ is required and for the calculation of $V'_{\mathbf{g}}$ one needs the so-called absorptive form factor $f'(\mathbf{g})$, which is also an atomic quantity. If one has a simple procedure to evaluate these quantities for every atom, one can very efficiently calculate $V_{\mathbf{g}}$ and $V'_{\mathbf{g}}$ for every crystal.

The elastic scattering amplitudes are well known and standard values have been published for $f(s)$, where $s = g/4\pi$ (e.g. Doyle & Cowley, 1974). Nowadays it is more convenient to use computer algorithms rather than tables to calculate scattering amplitudes. For this reason several attempts have been made to fit or interpolate the tabulated values. The classical fit function proposed by Doyle & Turner (1968) is a superposition of Gauss functions. As the asymptotic behaviour of the elastic form factor is proportional to s^{-2} , the Gaussian fit is very inaccurate for large values of s . In practice this fit should not be used for $s > 2 \text{ \AA}^{-1}$.

The determination of the absorptive form factor is more complicated since $f'(\mathbf{g})$ is given by the integral representation (Hall & Hirsch, 1965)

$$f'(\mathbf{g}) = (1/k) \int d^2 \mathbf{q} f(\mathbf{q}) f(\mathbf{q}-\mathbf{g}) (\exp[-Mg^2] - \exp\{-M[q^2 - (\mathbf{q}-\mathbf{g})^2]\}), \quad (6)$$

where k denotes the wavenumber of the incident electron and $\hbar\mathbf{q}$ is the momentum transferred to the crystal. The standard method is to perform this integration numerically. This has been done for example by Radi (1970) who published some values of $U_{\mathbf{g}}$ for a small variety of crystals. But in practice this is a very cumbersome method since the integration requires significant computing time. A practicable alternative has been proposed by Bird & King (1990). They calculated $f'(s)$ numerically on a grid of s and M values. The results are stored in a dataset and used to interpolate the values which are actually required. Another idea is to perform the integration analytically. This has been done by Buxton & Loveluck (1977). Their results are not very accurate since they used the interpolation formula of Doyle & Turner (1968) as an analytical representation for the elastic scattering amplitudes for all s .

We propose an empirical analytical expression for the scattering amplitudes which is well suited for our purposes. If one writes $f(s)$ as

$$f(s) = s^{-2} \sum_i A_i [1 - \exp(-B_i s^2)] \quad (7)$$

it is possible to fit the scattering amplitudes very accurately for all values of $s < \infty$. Moreover, the integration can be performed analytically allowing a fast evaluation of $f'(\mathbf{g})$.

The same type of formula can be obtained by applying the Mott formula to standard fit functions

for X-ray scattering amplitudes, which are given as a sum of Gauss functions plus a constant. We want to stress the point that X-ray fit functions must not be used, because electron scattering amplitudes computed by means of the Mott formula from X-ray scattering amplitudes are very inaccurate for small values of s (Peng & Cowley, 1988). We have avoided this problem by fitting the functions in (7) directly to the elastic scattering amplitudes for electrons.

2. The elastic scattering amplitudes

A reliable fit function should be precise for all values of s in the interval $[0, \infty]$. In order to obtain accurate values for the fitting coefficients we used the following two methods.

The function was fitted to the standard values of electron scattering amplitudes. For 58 atoms Doyle & Cowley (1974) have reported data for $s < 6 \text{ \AA}^{-1}$, for the remaining atoms data are available only for $s \leq 2 \text{ \AA}^{-1}$. For these atoms the missing values have been obtained by applying the Mott formula to the X-ray scattering amplitudes of Fox & O'Keefe (1989). As input to the fitting procedure we selected eighteen values at $s = 0.0, 0.1, 0.2, 0.3, 0.4, 0.5, 0.6, 0.8, 1.0, 1.4, 1.6, 1.8, 2.0, 2.5, 3.0, 4.0, 5.0, 6.0 \text{ \AA}^{-1}$. This selection ensures the correct behaviour of the fit function for $s \leq 6 \text{ \AA}^{-1}$.

To include the correct asymptotic behaviour of $f(s)$ for large values of s we consider that the elastic scattering amplitude is the Fourier transform of the electrostatic potential. Therefore the shape of $f(s)$ for large s depends on the potential near the nucleus. In this region the potential can be approximated by a screened Coulomb potential. Thus the asymptotic behaviour of the scattering amplitude for large s is Lorentzian and can be written as

$$\lim_{s \rightarrow \infty} f(s) = 0.02395Z \text{ \AA}^{-1} / (s^2 + \alpha^2), \quad (8)$$

where α is a function of the screening length. We observed that the simplified form

$$f(s) = 0.02395Z \text{ \AA}^{-1} / s^2 \quad (9)$$

is a good approximation of the tabulated values at $s = 6 \text{ \AA}^{-1}$. Since the asymptotic behaviour for large s of our fit function is given by

$$\lim_{s \rightarrow \infty} f(s) = s^{-2} \sum_i A_i \quad (10)$$

the coefficients A_i must fulfil the condition

$$\sum_i A_i = 0.02395Z \text{ \AA}^{-1} \quad (11)$$

to obtain the correct asymptotic shape.

The calculations have shown that seven fit parameters are sufficient for a good approximation. The

corresponding fit function is given by

$$f(s) = s^{-2} \sum_{i=1}^6 A_i [1 - \exp(-B_i s^2)] \quad (12)$$

where

$$A_1 = A_2 = A_3, \quad A_4 = A_5 = A_6 \quad (13)$$

and, in order to fulfil (11),

$$A_1 = 0.02395Z \text{ \AA}^{-1} / 3(1 + V), \quad A_4 = VA_1. \quad (14)$$

The seven parameters B_i ($i = 1, \dots, 6$) and V have been subjected to the fitting procedure. The results which are given in Table 1 show that the maximum relative error is smaller than 4% for all elements except He and Li. In order to give some characteristic examples the fit functions for Mg and O are depicted in Fig. 1.

3. The absorptive form factor

The specific representation of the elastic scattering amplitudes given in (5) allows an analytical evaluation of the absorptive form factor. The resulting formula which has been implemented in the Fortran subroutine *FSCATT* is given in the Appendix. The details of the calculation are given elsewhere (Weickenmeier, 1990).

To check the accuracy of our calculation a comparison of our results with some theoretical and experimental values is shown in Table 2. Bird & King (1990) used the same elastic scattering amplitudes to compute the absorptive form factor. Therefore the two results show excellent agreement. The values derived by Radi (1970) are somewhat different because he used non-relativistic scattering amplitudes computed from a Hartree-Fock-Slater atomic model. The comparison of the theoretical and experimental results demonstrates that the rough approximation of the Einstein model yields useful estimates for $V'_{\mathbf{g} \neq 0}$, except for Cu and Au. The latter discrepancies cannot be explained by erroneous $\langle u^2 \rangle$ data because these have hardly changed since Radi's paper appeared (*cf.* Schober & Dederichs, 1981).

Large discrepancies occur for V'_0 . This behaviour is not surprising since V'_0 is largely dominated by plasmon scattering, whereas we have only considered TDS. However, since V'_0 attenuates all reflections in exactly the same way, it does not affect the relative intensity of the Bragg spots.

4. Subroutine *FSCATT*

This subroutine which has been programmed in standard Fortran77 is specified as the complex function *FSCATT*(G, UL, Z, SYMBOL, ACCVLT, ABSFLG, ACCFLG, DWFLG).

Table 1. *The fitting coefficients for the elastic scattering amplitudes as defined in (10), (11) and (12)*

The units of B_i are \AA^2 , the units of s are \AA^{-1} . The maximum relative error e of the fit function given in percent is shown in the last column and in the last but one column the s value where it occurs.

Z	Symbol	V	B_1	B_2	B_3	B_4	B_5	B_6	s	e
2	He	0.5	2.542E+00	8.743E+00	1.269E+01	4.371E-01	5.294E+00	2.825E+01	3.0	6.2
3	Li	0.5	6.845E-01	3.065E+00	6.240E+00	1.262E+02	1.312E+02	1.318E+02	2.5	4.2
4	Be	0.3	5.400E-01	3.388E+00	5.562E+01	5.078E+01	6.701E+01	9.637E+01	3.0	3.4
5	B	0.5	3.314E-01	2.975E+00	3.401E+01	3.598E+01	3.668E+01	6.081E+01	1.8	2.4
6	C	0.5	2.946E-01	3.934E+00	2.498E+01	2.528E+01	2.547E+01	4.670E+01	0.8	2.4
7	N	0.5	2.393E-01	4.935E+00	1.812E+01	1.570E+01	1.582E+01	4.024E+01	2.5	2.0
8	O	0.5	6.376E+00	8.037E+00	2.721E+01	1.116E-01	3.869E-01	1.090E+01	3.0	1.7
9	F	0.5	2.180E-01	6.770E+00	7.051E+00	6.675E+00	1.238E+01	2.808E+01	1.0	1.7
10	Ne	0.5	2.006E-01	5.498E+00	6.281E+00	7.192E+00	7.548E+00	2.326E+01	1.0	2.7
11	Na	0.5	2.190E-01	5.300E+00	5.319E+00	5.283E+00	5.285E+00	1.282E+02	1.0	2.5
12	Mg	0.5	1.976E+00	2.809E+00	1.639E+01	5.494E-02	2.061E+00	1.217E+02	0.3	2.2
13	Al	0.4	2.297E+00	2.358E+00	2.499E+01	7.462E-02	5.595E-01	1.285E+02	3.0	2.8
14	Si	0.5	1.737E+00	3.043E+00	3.057E+01	5.070E-02	9.918E-01	8.618E+01	2.5	1.4
15	P	0.5	1.795E-01	2.632E+00	2.676E+00	3.457E+01	3.678E+01	5.406E+01	1.4	3.6
16	S	0.5	1.006E+00	4.904E+00	3.135E+01	3.699E-02	9.870E-01	4.494E+01	3.0	2.0
17	Cl	0.5	1.846E-01	1.480E+00	5.210E+00	2.479E+01	3.206E+01	3.910E+01	1.6	3.4
18	Ar	0.5	2.006E-01	6.533E+00	2.272E+01	1.200E+00	1.274E+00	3.626E+01	3.0	2.6
19	K	0.2	4.442E-01	3.367E+00	1.963E+01	1.824E-02	2.351E+01	2.129E+02	0.8	2.6
20	Ca	0.3	1.827E-01	2.066E+00	1.699E+01	1.158E+01	1.398E+01	1.861E+02	1.8	3.9
21	Sc	0.5	1.425E-01	1.466E+00	1.547E+01	4.243E+00	9.804E+00	1.215E+02	1.8	2.8
22	Ti	0.5	1.278E-01	1.456E+00	1.210E+01	4.617E+00	1.197E+01	1.050E+02	1.8	3.2
23	V	0.5	1.313E-01	1.399E+00	8.008E+00	7.981E+00	1.341E+01	9.531E+01	1.8	2.1
24	Cr	0.5	1.231E-01	2.384E+00	9.921E+00	1.648E+00	1.100E+01	6.846E+01	0.1	3.1
25	Mn	0.5	4.817E-01	3.783E+00	8.473E+00	4.690E-02	8.745E+00	7.744E+01	2.5	1.4
26	Fe	0.5	4.470E-01	6.894E+00	6.903E+00	5.691E-02	3.026E+00	7.087E+01	0.1	1.3
27	Co	0.5	1.071E-01	3.636E+00	7.558E+00	1.280E+00	5.140E+00	6.716E+01	0.1	2.6
28	Ni	0.5	1.107E-01	1.619E+00	6.003E+00	5.975E+00	6.060E+00	5.941E+01	2.5	1.7
29	Cu	0.5	1.129E-01	1.891E+00	5.085E+00	5.073E+00	5.099E+00	4.639E+01	0.1	2.5
30	Zn	0.5	1.021E-01	1.734E+00	4.783E+00	4.807E+00	5.645E+00	5.122E+01	2.5	2.4
31	Ga	0.5	1.064E-01	1.537E+00	5.138E+00	4.743E+00	5.000E+00	6.143E+01	0.1	1.8
32	Ge	0.5	9.583E-02	1.677E+00	4.703E+00	2.912E+00	7.870E+00	6.494E+01	0.0	2.3
33	As	0.5	9.428E-02	2.214E+00	3.951E+00	1.521E+00	1.581E+01	5.241E+01	0.4	2.2
34	Se	0.5	9.252E-02	1.602E+00	3.049E+00	3.185E+00	1.894E+01	4.763E+01	2.5	1.7
35	Br	0.5	9.246E-02	1.773E+00	3.481E+00	1.884E+00	2.269E+01	4.069E+01	2.0	1.5
36	Kr	0.5	4.932E-01	2.083E+00	1.141E+01	3.333E-02	2.097E+00	4.238E+01	1.0	1.8
37	Rb	0.2	1.580E-01	1.715E+00	9.392E+00	1.675E+00	2.359E+01	1.525E+02	1.6	3.3
38	Sr	0.3	3.605E-01	2.128E+00	1.246E+01	1.526E-02	2.108E+00	1.332E+02	2.5	1.9
39	Y	0.5	9.003E-02	1.414E+00	2.053E+00	1.026E+01	1.075E+01	9.064E+01	0.1	3.3
40	Zr	0.5	1.009E-01	1.154E+00	2.347E+00	1.058E+01	1.095E+01	8.282E+01	0.0	2.4

The elastic scattering amplitude will be returned as the real part of FSCATT, the absorptive form factor as the imaginary part, respectively. Moreover, the atomic symbol SYMBOL will be returned. The input parameters are the modulus G of the reciprocal-

lattice vector \mathbf{g} , the root-mean-square value UL of the thermal displacement $\langle u^2 \rangle^{1/2}$, the atomic number Z and the acceleration voltage ACCVLT in kV. Three logical parameters have control functions. Only if ABSFLG is true will the absorptive form factor be

Table 1 (cont.)

Z	Symbol	V	B_1	B_2	B_3	B_4	B_5	B_6	s	e
41	Nb	0.5	9.243E-02	1.170E+00	5.940E+00	1.306E+00	1.343E+01	6.637E+01	0.1	2.7
42	Mo	0.5	4.354E-01	1.248E+00	7.454E+00	3.543E-02	9.914E+00	6.172E+01	0.1	2.2
43	Tc	0.5	4.594E-01	1.182E+00	8.317E+00	3.226E-02	8.323E+00	6.498E+01	0.1	1.9
44	Ru	0.4	8.603E-02	1.396E+00	1.170E+01	1.396E+00	3.452E+00	5.556E+01	2.5	3.7
45	Rh	0.5	9.214E-02	1.113E+00	7.658E+00	1.126E+00	8.325E+00	4.838E+01	1.8	2.2
46	Pd	0.5	9.005E-02	1.125E+00	9.698E+00	1.085E+00	5.709E+00	3.349E+01	2.0	2.3
47	Ag	0.5	8.938E-02	3.191E+00	9.100E+00	8.090E-01	8.144E-01	4.134E+01	2.0	2.4
48	Cd	0.3	2.885E-01	1.613E+00	8.997E+00	1.711E-02	9.467E+00	5.813E+01	3.0	1.6
49	In	0.4	8.948E-02	1.233E+00	8.231E+00	1.224E+00	7.062E+00	5.970E+01	2.0	2.5
50	Sn	0.6	7.124E-02	8.553E-01	6.401E+00	1.336E+00	6.382E+00	5.092E+01	2.5	2.5
51	Sb	0.6	3.575E-01	1.325E+00	6.517E+00	3.550E-02	6.519E+00	5.081E+01	0.0	1.2
52	Te	0.6	5.009E-01	3.953E+00	7.628E+00	3.005E-02	5.074E-01	4.963E+01	0.1	0.6
53	I	0.4	8.429E-02	1.130E+00	8.862E+00	1.130E+00	9.132E+00	5.602E+01	2.5	2.5
54	Xe	0.4	2.780E-01	1.621E+00	1.145E+01	2.032E-02	3.275E+00	5.144E+01	1.4	1.4
55	Cs	0.1	1.204E-01	1.537E+00	9.816E+00	4.122E+01	4.262E+01	2.243E+02	1.8	2.9
56	Ba	0.1	1.223E-01	1.449E+00	9.502E+00	4.941E+01	7.495E+01	2.170E+02	1.8	2.6
57	La	0.3	8.930E-02	1.262E+00	8.097E+00	1.203E+00	1.766E+01	1.166E+02	2.5	2.9
58	Ce	0.3	8.504E-02	1.283E+00	1.122E+01	1.327E+00	4.610E+00	1.122E+02	2.5	3.2
59	Pr	0.2	9.805E-02	1.526E+00	8.590E+00	1.239E+00	2.249E+01	1.400E+02	2.5	3.0
60	Nd	0.2	9.413E-02	1.266E+00	5.988E+00	1.779E+01	1.814E+01	1.326E+02	2.5	3.3
61	Pm	0.2	9.447E-02	1.251E+00	5.912E+00	1.629E+01	1.673E+01	1.279E+02	2.5	3.1
62	Sm	0.2	9.061E-02	1.593E+00	1.064E+01	1.789E+00	2.221E+00	1.246E+02	2.5	3.3
63	Eu	0.1	1.049E-01	1.544E+00	8.652E+00	7.093E+00	5.337E+01	1.837E+02	2.5	2.7
64	Gd	0.2	9.338E-02	1.387E+00	7.359E+00	1.551E+00	2.082E+01	1.110E+02	2.5	2.2
65	Tb	0.1	1.019E-01	1.524E+00	7.169E+00	2.086E+01	4.929E+01	1.661E+02	2.5	2.7
66	Dy	0.2	8.402E-02	1.409E+00	7.140E+00	1.348E+00	1.142E+01	1.080E+02	3.0	2.7
67	Ho	0.1	9.441E-02	1.618E+00	6.271E+00	4.035E+01	4.283E+01	1.306E+02	2.5	2.9
68	Er	0.2	8.211E-02	1.251E+00	4.812E+00	1.084E+01	1.090E+01	1.001E+02	2.5	2.6
69	Tm	0.1	9.662E-02	1.602E+00	5.675E+00	3.059E+01	3.113E+01	1.387E+02	2.0	2.4
70	Yb	0.1	9.493E-02	1.602E+00	5.439E+00	2.831E+01	2.928E+01	1.381E+02	2.0	2.6
71	Lu	0.1	9.658E-02	1.568E+00	5.322E+00	3.418E+01	3.525E+01	1.214E+02	1.8	2.3
72	Hf	0.1	9.294E-02	1.555E+00	5.251E+00	3.752E+01	3.888E+01	1.052E+02	1.8	2.6
73	Ta	0.4	6.298E-02	8.195E-01	2.891E+00	5.543E+00	5.981E+00	5.442E+01	0.1	2.5
74	W	0.2	7.902E-02	1.371E+00	8.234E+00	1.383E+00	1.392E+00	7.712E+01	2.5	2.3
75	Re	0.5	5.266E-02	9.072E-01	4.438E+00	9.459E-01	4.375E+00	4.398E+01	0.2	2.3
76	Os	0.4	2.270E-01	1.570E+00	6.345E+00	1.564E-02	1.618E+00	4.616E+01	0.1	1.5
77	Ir	0.5	5.055E-02	8.677E-01	5.093E+00	8.812E-01	3.569E+00	3.977E+01	3.0	2.2
78	Pt	0.5	5.253E-02	8.377E-01	3.959E+00	8.152E-01	6.442E+00	3.421E+01	0.0	1.8
79	Au	0.4	5.493E-01	1.728E+00	6.720E+00	2.637E-02	7.253E-02	3.546E+01	0.2	1.1
80	Hg	0.4	2.194E-01	1.416E+00	6.682E+00	1.472E-02	1.576E+00	3.716E+01	0.2	1.2

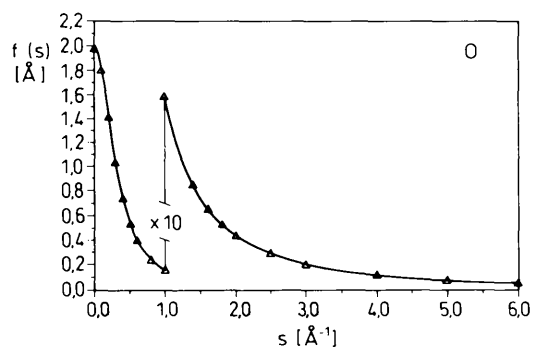
calculated. Both the elastic scattering amplitude and the absorptive form factor depend on the acceleration voltage. For a given acceleration voltage the former must be multiplied by the relativistic factor γ , the latter by γ^2/k . If ACCFLG is true, this will be done. DWFLG controls whether or not the elastic scattering

amplitude should be multiplied by the Debye-Waller factor $\exp(-Mg^2)$.

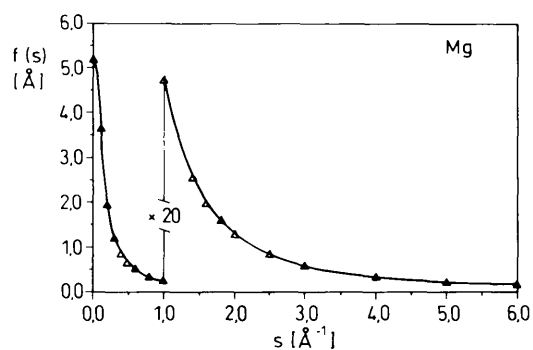
The program has about 550 lines of source code and the size is less than 20 kbytes. Only single precision is used. There are no special hardware requirements.

Table 1 (cont.)

Z	Symbol	V	B_1	B_2	B_3	B_4	B_5	B_6	s	e
81	Tl	0.4	2.246E-01	1.128E+00	4.303E+00	1.485E-02	7.156E+00	4.309E+01	0.1	1.9
82	Pb	0.3	6.432E-02	1.194E+00	7.393E+00	1.142E+00	1.289E+00	5.113E+01	2.5	1.8
83	Bi	0.4	5.380E-02	8.672E-01	1.875E+00	7.648E+00	7.868E+00	4.564E+01	3.0	1.9
84	Po	0.4	5.011E-01	1.638E+00	6.786E+00	2.187E-02	8.602E-02	4.673E+01	0.1	1.0
85	At	0.4	2.232E-01	1.108E+00	3.591E+00	1.011E-02	1.164E+01	4.507E+01	3.0	1.2
86	Rn	0.4	2.115E-01	1.140E+00	3.415E+00	1.188E-02	1.341E+01	4.311E+01	1.8	1.1
87	Fr	0.1	9.435E-02	1.026E+00	6.255E+00	3.251E+01	3.629E+01	1.491E+02	2.0	3.1
88	Ra	0.2	7.300E-02	1.018E+00	5.896E+00	1.031E+00	2.037E+01	1.153E+02	2.0	2.9
89	Ac	0.2	7.515E-02	9.494E-01	3.725E+00	1.758E+01	1.975E+01	1.091E+02	2.0	2.8
90	Th	0.3	6.385E-02	9.019E-01	4.657E+00	9.025E-01	1.571E+01	8.370E+01	0.1	2.2
91	Pa	0.2	7.557E-02	8.492E-01	4.010E+00	1.695E+01	1.779E+01	1.002E+02	2.0	2.7
92	U	0.2	7.142E-02	1.149E+00	9.212E+00	9.592E-01	1.203E+00	1.043E+02	2.5	2.4
93	Np	0.2	6.918E-02	9.810E-01	5.954E+00	9.909E-01	2.206E+01	9.098E+01	2.5	3.0
94	Pu	0.2	7.136E-02	9.577E-01	6.132E+00	9.744E-01	1.567E+01	8.987E+01	2.5	2.7
95	Am	0.2	7.301E-02	9.327E-01	6.348E+00	9.103E-01	1.326E+01	8.686E+01	2.5	2.4
96	Cm	0.3	5.778E-02	7.227E-01	3.011E+00	9.219E+00	9.534E+00	6.587E+01	0.1	3.2
97	Bk	0.2	7.088E-02	7.759E-01	6.143E+00	1.790E+00	1.512E+01	8.357E+01	0.1	3.1
98	Cf	0.3	6.164E-02	8.136E-01	6.562E+00	8.381E-01	4.189E+00	6.141E+01	2.5	2.4



(a)



(b)

Fig. 1. A comparison of the fitted elastic scattering amplitudes $f(s)$ (solid lines) and the tabulated values (triangles) of Doyle & Cowley (1974) for (a) oxygen and (b) magnesium.

The source code can be obtained by electronic mail without any charge by contacting the mail address XLTOA6L@DDATHD21.BITNET. Otherwise the program is distributed on a $5\frac{1}{4}$ in floppy disk for IBM PCs or compatibles running under MS-DOS. In this case there will be a small charge of US \$20 to cover postage and handling.

5. Concluding remarks

We have shown that the Fourier coefficients $U_{\mathbf{g}}$ of the lattice potential can be calculated using only a small set of fitting parameters. Thermal diffuse scattering has been taken into account, while the influence of plasmon scattering and core excitation has been ignored. A crystal model has been used which disregards solid-state effects on the electrostatic potentials of the crystal atoms and ignores correlation between the thermal motions of the individual scatterers. Despite this neglect the elastic scattering part $V_{\mathbf{g}}$ of $U_{\mathbf{g}}$ is obtained very accurately and a reliable estimate of the absorptive part $V'_{\mathbf{g}}$ is found in most cases. Because any improvement would require extensive calculations the Einstein model is the state of the art. Up to now even the evaluation of this model has been tedious. Our calculation procedure, which has been implemented in a Fortran subroutine, allows a very efficient evaluation of both $V_{\mathbf{g}}$ and $V'_{\mathbf{g}}$. With this procedure the calculation of electron diffraction patterns will be more precise than those computed by previous methods.

Table 2. *A comparison of theoretical and experimental data for the absorptive part V'_g for different crystals*

The acceleration voltage is 100 kV, the temperature is 300 K. Column 1 shows the material, column 2 the hkl indices of the reciprocal-lattice vector \mathbf{g} , columns 3-8 the results for V'_g in eV. The data are taken from (1) present work; (2) Bird & King (1990); (3) Radi (1970); (4) Hashimoto (1964); (5) Reimer & Wächter (1980); (6) Doyle (1970); (7) Goringe (1966); (8) Renard, Croce, Gandais & Sauvin (1971); (9) Meyer-Ehmsen (1969); (10) Goodman & Lehmpfuhl (1967); (11) Gaukler & Graff (1970). References 4-11 were taken from Reimer (1984). The values of $\langle u^2 \rangle$ are the same as those used by Radi (1970); $\langle u^2 \rangle$ (\AA^{-2}) = 0.015 (Al), 0.0069 (Cu), 0.0074 (Au), 0.0045 (Si), 0.0091 (Ge), 0.0038 (MgO) and 0.019 (NaCl).

		Theory			Experiment		
Al	000	0.19 ¹	0.20 ²	0.16 ³	0.37 ⁴	0.60 ⁵	0.54 ⁶
	111	0.17 ¹	0.17 ²	0.15 ³	0.23 ⁴	0.17 ⁶	
	220	0.14 ¹	0.15 ²	0.13 ³	0.11 ⁵		
	311	0.13 ¹	0.13 ²	0.12 ³	0.13 ⁵		
Cu	000	0.88 ¹	0.89 ²	0.75 ³	1.48 ⁷	1.35 ⁵	
	111	0.82 ¹	0.81 ²	0.71 ³	0.81 ⁷		
	200	0.80 ¹	0.79 ²	0.70 ³	0.92 ⁷		
	220	0.72 ¹	0.71 ²	0.64 ³	0.49 ⁵		
	311	0.66 ¹	0.66 ²	0.60 ³	0.45 ⁵		
Au	000	3.45 ¹	3.43 ²	3.04 ³	2.64 ⁸		
	220	2.93 ¹	2.91 ²	2.73 ³	2.00 ⁸		
	331	2.38 ¹	2.37 ²	2.27 ³	1.62 ⁵		
	440	1.90 ¹	1.89 ²	1.86 ³	1.50 ⁸		
Si	000	0.12 ¹	0.10 ³		0.68 ⁹	0.62 ⁵	
	220	0.10 ¹	0.09 ³		0.11 ⁹	0.14 ⁵	
	311	0.07 ¹	0.06 ³		0.08 ⁹	0.08 ⁵	
	422	0.09 ¹	0.08 ³		0.08 ⁹		
Ge	000	0.71 ¹	0.53 ³		1.25 ⁹		
	220	0.63 ¹	0.49 ³		0.52 ⁹		
	400	0.56 ¹	0.45 ³				
	422	0.50 ¹	0.42 ³		0.36 ⁹		
MgO	000	0.13 ¹	0.10 ³		1.50 ¹⁰		
	200	0.11 ¹	0.10 ³		0.13 ¹⁰		
NaCl	000	0.23 ¹	0.20 ³				
	200	0.19 ¹	0.17 ³		0.21 ¹¹		
	420	0.14 ¹			0.15 ¹¹		

We thank Professor H. Rose for valuable discussions. One of the authors (HK) is indebted to several colleagues (Professor D. van Dyck, Professor H. Lichte, Professor K. Urban, Dr P. Stadelmann) for suggesting the problem to him. Support by the Stiftung Volkswagenwerk is gratefully acknowledged.

APPENDIX

Here we want to present the result for the absorptive form factor. By inserting (7) in (6) we obtain

$$f'(g) = k^{-1} \sum_{i,j} A_i A_j [\exp(-Mg^2) I_{ij}^1(g) + I_{ij}^2(M, g)], \quad (15)$$

with the abbreviations

$$I_{ij}^1(g) = \int [d^2\mathbf{q}/q^2(\mathbf{q}-\mathbf{g})^2] \times \{1 - \exp[-B_i q^2] - \exp[-B_j(\mathbf{q}-\mathbf{g})^2] + \exp[-B_i q^2 - B_j(\mathbf{q}-\mathbf{g})^2]\}. \quad (16)$$

$$I_{ij}^2(M, g) = \int [d^2\mathbf{q}/q^2(\mathbf{q}-\mathbf{g})^2] (\exp\{-M[q^2 + (\mathbf{q}-\mathbf{g})^2]\} - \exp[-(B_i + M)q^2 - M(\mathbf{q}-\mathbf{g})^2] - \exp[-Mq^2 - (B_j + M)(\mathbf{q}-\mathbf{g})^2] + \exp[-(B_i + M)q^2 - (B_j + M)(\mathbf{q}-\mathbf{g})^2]). \quad (17)$$

The integration yields the following expressions:

$\mathbf{g} = 0$:

$$I_{ij}^1(g) = \pi \left\{ B_i \ln \frac{B_i + B_j}{B_i} + B_j \ln \frac{B_i + B_j}{B_j} \right\} \quad (18)$$

$$I_{ij}^2(M, g) = \pi \left\{ (B_i + 2M) \ln \frac{B_i + B_j + 2M}{B_i + 2M} + B_j \ln \frac{B_i + B_j + 2M}{B_j + 2M} + 2M \ln \frac{2M}{B_j + 2M} \right\}. \quad (19)$$

$\mathbf{g} \neq 0$:

$$I_{ij}^1(g) = (\pi/g^2) \left\{ 2C + \ln(B_i g^2) + \ln(B_j g^2) - 2\text{Ei}\left(-\frac{B_i B_j}{B_i + B_j} g^2\right) + \exp[-B_i g^2] \times \left[\text{Ei}\left(\frac{B_i^2}{B_i + B_j} g^2\right) - \text{Ei}(B_i g^2) \right] + \exp[-B_j g^2] \times \left[\text{Ei}\left(\frac{B_j^2}{B_i + B_j} g^2\right) - \text{Ei}(B_j g^2) \right] \right\} \quad (20)$$

$$I_{ij}^2(M, g) = \frac{\pi}{g^2} \left\{ 2\text{Ei}\left[-\frac{M(B_i + M)}{B_i + 2M} g^2\right] + 2\text{Ei}\left[-\frac{M(B_j + M)}{B_j + 2M} g^2\right] - 2\text{Ei}\left[-\frac{(B_i + M)(B_j + M)}{B_i + B_j + 2M} g^2\right] - 2\text{Ei}\left(-\frac{1}{2}Mg^2\right) + \exp[-Mg^2] \times \left[2\text{Ei}\left(\frac{1}{2}Mg^2\right) - \text{Ei}\left(\frac{M^2}{B_i + 2M} g^2\right) - \text{Ei}\left(\frac{M^2}{B_j + 2M} g^2\right) \right] + \exp[-(B_i + M)g^2] \times \left\{ \text{Ei}\left[\frac{(B_i + M)^2}{B_i + B_j + 2M} g^2\right] - \text{Ei}\left[\frac{(B_i + M)^2}{B_i + 2M} g^2\right] \right\} + \exp[-(B_j + M)g^2] \times \left\{ \text{Ei}\left[\frac{(B_j + M)^2}{B_i + B_j + 2M} g^2\right] - \text{Ei}\left[\frac{(B_j + M)^2}{B_j + 2M} g^2\right] \right\} \right\}. \quad (21)$$

Here $Ei(x)$ denotes the exponential integral function defined as

$$x < 0: \quad Ei(x) = \int_{-\infty}^x (e^t/t) dt$$

$$x > 0: \quad Ei(x) = -\lim_{\epsilon \rightarrow 0} \left(\int_{-x}^{-\epsilon} + \int_{\epsilon}^{\infty} \right) (e^{-t}/t) dt \quad (22)$$

and $C = 0.577215 \dots$ is the Euler constant.

References

- BIRD, D. M. & KING, Q. A. (1990). *Acta Cryst.* **A46**, 202–208.
 BUXTON, B. F. & LOVELUCK, J. E. (1977). *J. Phys. C*, **10**, 3941–3958.
 DOYLE, P. A. (1970). *Acta Cryst.* **A26**, 133–139.
 DOYLE, P. A. & COWLEY, J. M. (1974). *International Tables for X-ray Crystallography*, Vol. IV, pp. 152–174. Birmingham: Kynoch Press. (Present distributor Kluwer Academic Publishers, Dordrecht.)
 DOYLE, P. A. & TURNER, P. S. (1968). *Acta Cryst.* **A24**, 390–397.
 FOX, A. G. & O'KEEFE, M. A. (1989). *Acta Cryst.* **A45**, 786–793.
 GAUKLER, K. G. & GRAFF, K. (1970). *Z. Phys.* **232**, 190–204.
 GOODMAN, P. & LEHMPPFUHL, G. (1967). *Acta Cryst.* **22**, 14–24.
 GORINGE, M. J. (1966). *Philos. Mag.* **14**, 93–97.
 HALL, C. R. & HIRSCH, P. B. (1965). *Proc. R. Soc. London Ser. A*, **286**, 158–177.
 HASHIMOTO, H. (1964). *J. Appl. Phys.* **35**, 277–290.
 HASHIMOTO, H., HOWIE, A. & WHELAN, M. J. (1962). *Proc. R. Soc. London Ser. A*, **269**, 80–103.
 MEYER-EHMSEN, G. (1969). *Z. Phys.* **218**, 352–377.
 PENG, L.-M. & COWLEY, J. M. (1988). *Acta Cryst.* **A44**, 1–5.
 RADI, G. (1970). *Acta Cryst.* **A26**, 41–56.
 REIMER, L. (1984). *Transmission Electron Microscopy*, pp. 295–300. Berlin: Springer.
 REIMER, L. & WÄCHTER, M. (1980). In *Electron Microscopy*, Vol. 3, edited by P. BREDEROO & G. BOOM, pp. 192–193. Leiden: Seventh European Congr. Electron Microscopy Foundation.
 RENARD, D., CROCE, P., GANDAIS, M. & SAUVIN, M. (1971). *Phys. Status Solidi B*, **47**, 411–421.
 ROSSOUW, C. J. & BURSILL, L. A. (1986). *Proc. R. Soc. London Ser. A*, **408**, 149–164.
 SCHÖBER, H. R. & DEDERICHS, P. H. (1981). In *Landolt-Börnstein: Numerical Data and Functional Relationships in Science and Technology*, edited by K.-H. HELLWEGE & J. L. OLSEN, Group III, Vol. 13a, pp. 1–191. Berlin: Springer.
 STEEDS, J. W. (1983). In *Quantitative Electron Microscopy*, edited by J. N. CHAPMAN & A. J. CRAVEN, pp. 49–96. Glasgow: Scottish Univs. Summer School in Physics.
 WEICKENMEIER, A. (1990). In preparation.
 YOSHIOKA, H. (1957). *J. Phys. Soc. Jpn*, **12**, 618–628.

Acta Cryst. (1991). **A47**, 597–604

The Interpretation of Raw Diffractometer Data

BY A. T. H. LENSTRA, H. J. GEISE AND F. VANHOUTEGHEM†

University of Antwerp (UIA), Department of Chemistry, Universiteitsplein 1, B-2610 Wilrijk, Belgium

(Received 27 July 1990; accepted 26 April 1991)

Abstract

Statistical analysis reveals that the X-ray background rigorously follows a counting statistical distribution provided the measurements are made under truly fixed-time conditions in a small $(\sin \theta)/\lambda$ interval. The operational procedures to ensure this are not trivial. First, the design of, for example, the Enraf-Nonius CAD-4 diffractometer is such that measurements made at constant scan speed at different Bragg angles may have somewhat different measuring times. Failure to correct for this leads primarily to an increase in the variance of the data. Second, the use of a rapid prescan followed, when appropriate, by a slower main scan leads to a set of prescan data biased towards overestimates of background values and underestimates of raw intensities. The effort needed to extract from the data unbiased estimates of averages and variances of the X-ray background is rewarding. It can lead to a lowering of the standard

deviation of a net intensity by up to one order of magnitude. This in turn means that many more intensities of weak reflections are reliably estimated and are hence worth including in the structure determination. This obviously leads to increased model accuracy. An example is given. A change in measuring procedure is recommended which will increase the efficiency of the standard background-peak-background procedure.

Introduction

The present standard data-reduction procedure operates on each reflection measurement separately and thus completely ignores any knowledge that might have been acquired prior to the current measurement. This is surprising considering the great impact ascribed to experience in all aspects of life. More specifically, statistical methods are available to separate the effects of random measurement errors from systematic factors, as well as to extract from data sets information which can be used to judge the quality

† Deceased 23 January 1991.